

# Sparse optical sampling in the close proximity of a robotic arm

Martin Laurenzis<sup>1</sup>, Ante Marić<sup>2</sup>, Emmanuel Bacher<sup>1</sup>, Mateusz Pietrzak<sup>1</sup>,  
Stéphane Schertzer<sup>1</sup>, Francesco Grella<sup>3</sup>, and Sylvain Calinon<sup>2</sup>

<sup>1</sup> French-German Research Institute of Saint-Louis (ISL), 68301 Saint-Louis, France  
martin.laurenzis@isl.eu,

WWW home page: <https://www.isl.eu>

<sup>2</sup> Idiap Research Institute, CH-1920 Martigny, Switzerland

<sup>3</sup> DIBRIS, University of Genoa, 16145 Genoa, Italy

**Abstract.** Close collaboration between humans and robots needs a sensing infrastructure to monitor the robot environment and secure human-robot interaction. In this context, we investigate sparse optical range sampling using a distributed network of robot mounted Time-of-Flight (ToF) sensors. We present an evaluation of sensor candidates, provide experimental characterization of an early prototype and show strategies for environment modeling and object reconstruction.

**Keywords:** sensor arrays and networks; robotic environment; proximity sensors; signed distance fields

## 1 Introduction

The effectiveness of Human-Robot Collaboration (HRC) strongly depends on the perceptual capabilities of the involved robotic system. To improve task performances and overall safety, a sensing architecture containing external ( $E1$ ,  $E2$ ) and robotic/robot-mounted ( $R1$ ,  $R2$ ,  $R3$ ) sensors can enhance the robotic awareness, see Fig. 1(a). But, as shown in Fig.1 (b), external sensors can suffer from

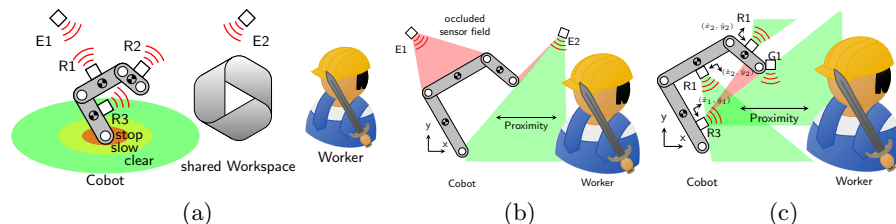


Fig. 1: Safe collaboration of human and robot in a production line can be realized, for instance, by (a) a Cobot equipped with (b) external ( $E1$ ,  $E2 \dots$ ) or (c) robot mounted ( $R1$ ,  $R2 \dots$ ) sensors.

Table 1: Non exhaustive list of optical time-of-flight proximity sensors with light detection and ranging (LIDAR) on integrated circuits (LoIC).

	Role	Manufacturer	Model	Package	Sensor			Laser	
		Name	No.	Type	ToF	Type	Resol.	Range	Type
Proximity		STMicro.	VL53L8	LoC	pulsed SPAD	$8 \times 8$	4 m	on chip	940
		OSRAM	TMF8828	LoC	pulsed SPAD	$8 \times 8$	4 m	on chip	940
		SHARP	GP2APx	LoC	pulsed SPAD	$1 \times 1$	1.2 m	on chip	940
		OnSemi	MicroFC	Sensor	pulsed SiPM	$1 \times 1$	10 m	sep.	905

occlusions and blind spots as well as from the need of a perfect calibrated environment. Especially in close proximity of robot and human, the occlusion of the line of sight can have critical consequences. Alternatively, industrial robots can be equipped with additional sensors that are integrated directly into the robotic platform (Fig.1 (c)).

A distributed network of sensors can cover the robot body and allow the proximity of the robot to be analyzed. In the current paper we neglect tactile sensing and investigate a network of distributed laser ranging sensors (LIDAR), as in [1], [2], [3]. The presented work was carried out within the SESTOSENSTO project (HORIZON-CL4-Digital-Emerging Grant 101070310). This work reports the collaborative work of multiple partners within the consortium. Further reading can be found online [4].

## 2 Optical range sampling in robot proximity

A task-oriented evaluation of optical range imaging sensors must be based on task-related constraints and, in addition to their physical performance, consider a hypothetical cost function  $S_{\text{SWAP-C}}(x)$ , that evaluates **Size**, **Weight** **And** electrical **Power** consumption as well as the sensor’s **Costs** (SWAP-C). Here, the sensor’s costs cover not only the economic trade value but incorporates also computational cost: data transfer loads and processing efforts.

*Proximity monitoring* has to cover the environment all around the robot within a hemisphere from very close (few centimeter) to, at least, the maximum range of the robotic arm. In this case, the optical resolution is initially of secondary importance, as it is only used for a rudimentary environmental model that is intended to distinguish open movement areas from fixed installations. In addition, and more important due to work safety issues, spatial coverage has to ensure reliable localization of human employees. Therefore, we decided to use a network of distributed sensors to provide complete coverage of the environment and avoid shadowing of areas by the robot itself.

Optical time-of-flight sensors are available in a compact size as LIDAR on integrated circuits (LoIC). In table 1 we provide an overview of a selection of LoIC candidates (green highlighted parameters meet requirements).

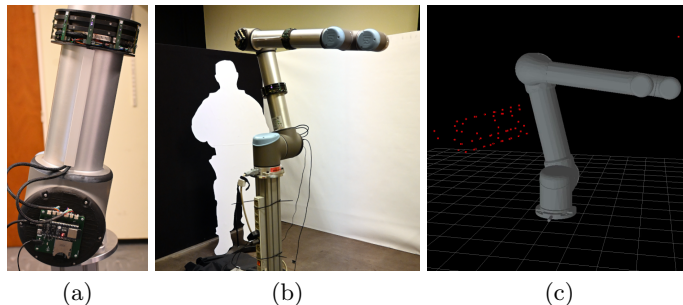


Fig. 2: Sensor network consisting of a bracelet with (a) 10 distributed LIDAR sensors and a micro-controller unit (MCU). The sensor is mounted on a robotic arm (b). The data of the robotic environment can be displayed (c) as a sparse point cloud.

### 3 Experimental evaluation

We have built an experimental setup to evaluate different sensors for proximity monitoring. The sensors were mounted on a robotic arm (UR10, Universal Robotics) and used in a synthetic scene consisting of a human silhouette and walls with light (white paper) and dark (black fabric) surfaces.

As illustrated in Fig. 2 (a), we set up networks of LoIC sensors in the form of a bracelet or waistband. Each unit consisted of 10 LoIC sensors and a micro-controller unit (MCU, Espressif, ESP32). The MCU is connected to the individual LoICs to control the automated data acquisition and to read out data. The bracelets were mounted on the individual robotic arm segments as illustrated in Fig. 2 (b). The recorded data is transmitted through a wireless network connection to a main processing unit (PC). High level data processing such as fusion and display of point clouds (Fig. 2 (c)), building an environment model (e.g. SLAM), the reconstruction of objects (Sec. 4), control and adaption of the robot motion as well as human robot interaction (HRI) will be realized on the main processing unit.

In our experiments, we used the LoICs TMF8828 (ams OSRAM) and VL53L8 (ST Microelectronics), respectively. Each individual sensor measures a point cloud of  $8 \times 8$  range values in a field of view of  $40^\circ \times 60^\circ$ . Thus, the group of 10 sensors cover a disk shaped area ( $360^\circ \times 40^\circ$ ) perpendicular to the arm segment. In this area, we were able to monitor the proximity of the robotic arm from close range (ca. 2 cm) to a maximal distance of about 3 m with a point cloud update rate of up to 5 Hz. The maximum range is impacted by the ambient light level which can alter the signal to noise level. Further the surface characteristics such as reflectance and orientation can effect the results. A detailed analysis is pending. Again, in our first approach we were able to cover a disk shaped area. In later application, the position (place and orientation) of the sensors mounted on the robot has to be optimized for maximal coverage and to comply with work task specific requirements.

## 4 Object reconstruction

Sampled distance information can be used to learn signed distance fields (SDFs) in order to reason about making contact with the environment or objects of interest. For this purpose, piecewise polynomial basis functions can be leveraged as an underlying model to represent continuous and smooth SDFs, with direct access to gradients. These properties make such representations directly usable for guiding movement in robotic manipulation tasks [5].

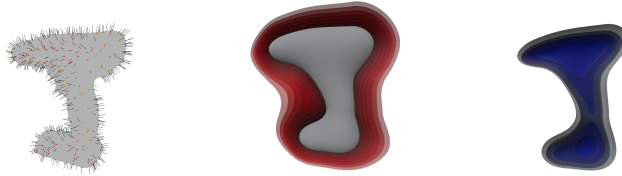


Fig. 3: Piecewise polynomial SDF of the 035\_power\_drill object from the YCB dataset [6]. The ground truth mesh with 700 non-uniformly distributed training samples is shown on the left. The center and right image show the reconstructed mesh and level sets (positive in red and negative in blue).

Fitting a piecewise polynomial SDF model amounts to learning a number of basis function weights from sampled distance data. A simple way of doing this is through least squares regression. Learning only from surface points and normals requires additional regularization terms in order to provide valid representations of distance [7]. In an online setting, data collected in batches or point-by-point can be used to update an arbitrary prior model through an incremental formulation of least squares [8]. Figure 3 shows an example object reconstruction. The training procedure for a 2D case is illustrated in Figure 4.

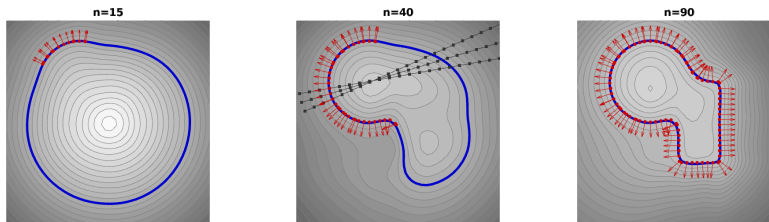


Fig. 4: Incremental learning of an SDF represented using piecewise polynomial basis functions, with level sets displayed as gray and blue contours. Starting from a spherical prior, the model is incrementally updated with  $n$  incoming samples, shown in red. Regularization is enforced on points shown in black.

## 5 Conclusions

We have evaluated different LoIC sensors to be used in a sensor network mounted on the robot skin. Our sensor networks can monitor the robot environment from close range several meters and sample a sparse point cloud which covers a disk shape area all around the robot arm without self occlusion or blind spots. In principle, these results comply with the requirements for a application in a safety and control system for human-robot-collaboration (HRC). Furthermore, we have investigated the reconstruction of object shapes from a small set of sample points. Our approach uses piecewise polynomial basis functions to implicitly represent shapes as signed distance fields (SDFs). Thus, without the need of a dense point cloud we are able to develop an environment model which can be used for further high level operations. Future developments foresee the design and implementation of a dedicated middleware architecture to provide efficient access to different proximity data representations. Moreover, the methods and technologies presented in this paper will be extended to real-world applications which are relevant for industrial manufacturing and agriculture scenarios.

## References

1. Francesco Giovinazzo, Francesco Grella, Marco Sartore, Manuela Adami, Riccardo Galletti, and Giorgio Cannata. From CySkin to ProxySKIN: Design, implementation and testing of a multi-modal robotic skin for Human-Robot Interaction. *Sensors*, 2024. submitted.
2. Satoshi Tsuji and Teruhiko Kohama. Proximity skin sensor using time-of-flight sensor for human collaborative robot. *IEEE Sensors Journal*, 19(14):5859–5864, 2019.
3. Odysseus Alexander Adamides, Anmol Saiprasad Modur, Shitij Kumar, and Ferat Sahin. A time-of-flight on-robot proximity sensing system to achieve human detection for collaborative robots. In *2019 IEEE 15th International Conference on Automation Science and Engineering (CASE)*, pages 1230–1236, 2019.
4. SestoSenso. <http://sestosenso.eu/>, 2023.
5. Yiming Li, Yan Zhang, Amirreza Razmjoo, and Sylvain Calinon. Learning robot geometry as distance fields: Applications to whole-body manipulation, 2023.
6. Berk Calli, Arjun Singh, James Bruce, Aaron Walsman, Kurt Konolige, Siddhartha Srinivasa, Pieter Abbeel, and Aaron M Dollar. Yale-cmu-berkeley dataset for robotic manipulation research. *Intl Journal of Robotics Research*, 36(3):261–268, 2017.
7. Gabriel Taubin. Smooth signed distance surface reconstruction and applications. In *Progress in Pattern Recognition, Image Analysis, Computer Vision, and Applications*, pages 38–45, 2012.
8. Ante Marić, Yiming Li, and Sylvain Calinon. Online learning of piecewise polynomial signed distance fields for manipulation tasks, 2024.